Comprehensive Summaries of Uppsala Dissertations
from the Faculty of Science and Technology 844

Growth Studies of SiC and BN:

from Theory and Experiment

BY

JENNY OLANDER

ACTA UNIVERSITATIS UPSALIENSIS
UPPSALA 2003

Dissertation at Uppsala University to be publicly examined in Häggsalen, Ångström Laboratory on Thursday the 5th of June, 2003 at 13:15 for the Degree of Doctor of Philosophy. The examination will be conducted in English.

Abstract
Olander, J. 2003. Growth Studies of SiC and BN: from Theory and Experiment.
Acta Universitatis Upsaliensis. *Comprehensive Summaries of Uppsala Dissertations from the Faculty of Science and Technology* 844. 44 pp. Uppsala. ISBN 91-554-6545-6.

Smaller cellular telephones and more energy-efficient windows are just two examples of technological advances which call for new materials. Materials chemists seek to develop new materials, both out of pure curiosity to see which combination of elements and structures can be obtained and in efforts to produce materials, with specific properties. The starting materials (in solid, liquid or gaseous form) can then be combined and prepared in various ways. A chemical method that is gaining more attention for thin-film growth is Atomic Layer Deposition (ALD). This is a sophisticated type of vapor deposition in which the precursor gases are introduced separately into the reaction chamber.

Silicon carbide (SiC) and cubic boron nitride (c-BN) are extremely hard diamond-like materials, both with a high potential for application within the modern microelectronics and tool industry. Hexagonal boron nitride (h-BN), with its graphite-like layered structure, is a promising ceramics material.

Deposition of thin SiC and BN films from gaseous precursors was studied by theoretical and experimental methods. The chemical composition and atomic arrangement of a growing surface is important for vapor growth. The surface may be terminated (e.g., by hydrogen atoms) and adopt various geometrical structures. Reconstruction of unterminated SiC(0001) surfaces, as well as H abstraction from the corresponding H-terminated surfaces, were studied using quantum mechanical calculations. Elementary reactions for vapor growth of SiC and BN, and *in situ* incorporation of dopant and contaminant species into these surfaces were also investigated theoretically. Moreover, thin films of BN were deposited by means of laser-assisted ALD. The general goal has been to predict and/or explain experimental results by investigating growth mechanisms.

Keywords: growth, quantum chemistry, DFT, ALD, laser-activation.

Jenny Olander, Department of Materials Chemistry. Uppsala University. Box 538, SE-751 21 Uppsala, Sweden.

ISBN 91-554-6545-6
ISSN 1104-232X
urn:nbn:se:uu:diva-3439 (http://urn.kb.se/resolve?urn=urn:nbn:se:uu:diva-3439)

List of Papers

This thesis is a summary of the following papers. Each article will be referred to by its Roman numeral.

I. **Influence of adsorbed species on the reconstruction of 4H-SiC(0001) surfaces**
J. Olander and K. M. E. Larsson; *J. Phys. Chem. B* 105 **(2001)**, 7619.

II. **An ab initio study of 4H-SiC(0001) surface processes at experimental temperatures**
J. Olander and K. M. E. Larsson; *Submitted for publication in J. Phys. Chem. B.*

III. **Ab initio calculation of adsorption to β-SiC Clusters**
J. Olander and K. M. E. Larsson; *J. Phys. Chem. B* 103 **(1999)**, 9604.

IV. **Initial growth of hexagonal and cubic boron nitride: A theoretical study**
J. Olander and K. M. E. Larsson; *Submitted for publication in Phys. Rev. B.*

V. **Laser-assisted ALD of BN thin films**
J. Olander and L. M. Ottosson and P. Heszler and J.-O. Carlsson and K. M. E. Larsson; *Submitted for publication in Thin Solid Films*.

VI. **Adsorption of N-containing species into SiC(0001) surfaces: A theoretical study**
J. Olander and K. M. E. Larsson; *Phys. Rev. B* 67 **(2003)**, 115306.

List of related Papers

The following articles are not included in the thesis.

VII. **Surface abstraction reactions at experimental temperatures: A theoretical study of 4H- SiC(0001)**
J. Olander and K. M. E. Larsson; *Mat. Sci. Forum* 353-356 **(2001)**, 231.

VIII. **Cubic boron nitride growth from NH_3 and BBr_3 precursors: A theoretical study**
J. Olander and K. M. E. Larsson; *Diam. Rel. Mat.* 11 **(2002)**, 1286.

IX. **Theoretical investigation of N-incorporation into SiC(0001) surfaces**
J. Olander and K. M. E. Larsson; *To appear in Mat. Sci. Forum, June 2003*.

Contents

Teoretiska och experimentella studier av kiselkarbid- och bornitridtillväxt

(Summary in Swedish)

För att kunna tillverka t. ex. mindre mobiltelefoner och effektivare solceller måste man ha tillgång till rätt utgångsmaterial. Ibland räcker inte befintliga material till för att uppnå det man skulle vilja. Dessutom kan formen av ett material behöva anpassas. Ett tunt skikt av ett välstrukturerat material kan exempelvis vara nödvändigt för en viss tillämpning. Materialkemister letar efter nya material, både av ren nyfikenhet på vilka elementkombinationer och strukturer som kan erhållas och på uppdrag att framställa material med specifika egenskaper.

Kiselkarbid (SiC) och kubisk bornitrid (c-BN) är diamantliknande material med många intressanta egenskaper. Båda materialen är extremt hårda och de besitter hög termisk och kemisk stabilitet. De är halvledare med breda bandgap som går att dopa både positivt och negativt. Dessa egenskaper gör att SiC och c-BN har flera (faktiska och potentiella) användningsområden inom modern mikroelektronik och verktygsindustri. Hexagonal bornitrid (h-BN) har helt andra egenskaper än den kubiska varianten. Den är exempelvis ett lovande kerammaterial p.g.a. sitt låga elektriska motstånd och sin utmärkta värmeledningsförmåga. Som korrosionsbeständigt smörjmedel kan det också användas som skyddande beläggning.

Det finns olika sätt att framställa nya material på. Man kan utgå från material i fast, flytande eller gasform. Utgångsmaterialen kan kombineras och prepareras på olika sätt. Tillverkningsprocesserna optimeras med avseende på temperatur, tryck och andra parametrar. För att kunna utvärdera resultaten måste man sedan analysera sina prov. Det gäller att ta reda på sammansättning, homogenitet, struktur, volym m.m. För att inte leta i blindo vill man ta reda på vilka mekanismer som leder till specifika resultat. Med hjälp av teoretisk modellering kan kemiska reaktionsmekanismer studeras på en nivå som är svår att uppnå experimentellt. Dessutom är teoretiska studier aldrig hälsovådliga och ofta ekonomiskt fördelaktiga. Arbetet som presenteras i den här avhandlingen har gått ut på att studera tillväxt av tunna skikt av SiC och BN utifån några olika aspekter. Studierna har främst genomförts med mycket noggranna kvantmekaniska beräkningar.

Partiklar kan börja växa i gasfasen innan de når ytan som de sedan beläggs

på. Som resultat kan nämnas att form och storlek hos partiklar av kubisk SiC starkt påverkar dessa tillväxtprocesser. Den kolrika (0001)-sidan av SiC har visat sig reagera mycket olikt motsvarande kiselrika sida när tillväxtmolekyler binder till den. Vidare så är det viktigt att kunna styra dopningsgraden under tillväxt för att erhålla material med önskade elektriska egenskaper. Kvävgas (N_2) har då visats vara mer trolig som kvävetillförande molekyl än ammoniak (NH_3) eller vätecyanid (HCN/HNC). Ett av målen med den här typen av teoretiska studier är generellt att förklara experimentella resultat genom att förstå mekanismerna bakom kemiska reaktioner. Dessutom kan reaktionerna i vissa fall förutsägas rent teoretisk och det är ju mycket fördelaktigt. Längdmåttet, som oftast används när man diskuterar bindningslängder är Ångström $\left(1\ \text{Å} = 0.1\ \text{nm (nanometer)} = 0.0000000001\ \text{m}\right)$. Som exempel är Si-C avståndet i SiC 1.89 Å.[1]

När det gäller bornitrid så undersöktes de inledande elementära reaktionerna för tillväxt utgående ifrån ammoniak (NH_3) och bortribromid (BBr_3). Sönderdelade fragment av NH_3 och BBr_3 visade sig då binda starkare till ytor av c-BN, respektive kanter av h-BN, än molekylerna själva. Bornitrid studerades även experimentellt. Tunna skikt av BN växtes med ALD (”Atomic Layer Deposition” eller ”tillväxt atomlager för atomlager”), utgående från NH_3 och BBr_3. För att tillföra extra energi till processen användes en ArF excimer laser som verkar vid 193 nm. Genom att stimulera gasen ovanför den växande BN-ytan med laserljus, sönderdelades utgångsmolekylerna till H, NH, NH_2, Br, B, BBr och BBr_2. Laseraktiveringen bidrog till en ökad tillväxthastighet och till ett något stabilare material vid lägre beläggningstemperaturer. Det resulterande materialet bestod av nanokristallina korn av hexagonal bornitrid. Skikten var jämna och dess tjocklek kunde styras med $\sim$1 nanometers nogrannhet.

[1] Uppsalaforskaren Anders Jonas Ångström (1814-1874), efter vilken denna enhet är uppkallad, har tillsammans med sin son Knut Ångström (1857-1910) namngett materialforskningslaboratoriet vid vilket denna avhandling är skriven.

Introduction

1.1 Properties

Silicon carbide (SiC) and the cubic modification of boron nitride (c-BN) are diamond-like materials with many interesting properties (Table 1.1). Because of their hardness, they are in analogy with diamond used as coating materials on cutting tools. Both SiC and c-BN are wide bandgap semiconductors which can either be *p*- or *n*-type doped, and they are chemically stable at high temperatures. These characteristics are, among others, valuable for applications within modern microelectronics and tool industry. The properties vary for the different SiC modifications and 4H-SiC is, for example, the preferred polytype for electronic purposes. However, the SiC polymorphs are not as fundamentally different as the cubic and hexagonal modifications of BN.

Hexagonal boron nitride (h-BN) is an insulating ceramics material with low electrical resistivity and high thermal conductivity. Similar to graphite, it has lubricating characteristics which makes it useful as a protective coating.

Table 1.1: Properties of different SiC- and BN-polymorphs [1, 2, 3, 4, 5].

Property	3C-SiC	4H-SiC	c-BN	h-BN
Structure	zink blende	wurtzite	zink blende	graphite-like
Unit cell parameter(s) [Å]	a=4.36	a=3.08	a=3.62	a=2.50
		c=10.08		c=6.66
Density [g/cm^3]	3.21	3.21	3.45	2.27
Hardness [Moh's]*	9.5	9.5	9.8	2
Bandgap [eV]	2.3	3.2	10.0	
Electron Mobility [cm^2/Vs]	750	800	-	-
Thermal Conductivity [W/K]	3-5	5-7	2-9	(a) 0.36
				(c) 0.68

*The hardness of diamond is 10 on Moh's scale.

1.2 Occurrence

Silicon carbide was first observed in 1824, by the Swedish scientist Berzelius, and this material has been used in cutting and grinding applications for more

than a hundred years [3]. In 1955 it could be produced for electronic purposes, but the growth still took place in an uncontrolled manner. Device quality epitaxial layers of SiC (grown by CVD) are commercially available today. However, the growth procedures of SiC still have to be improved in order to compete with silicon.

The research on BN is at present at a different stage compared to SiC research. Hexagonal boron nitride has been an important ceramic material for a long time, while cubic boron nitride only recently was industrially introduced (as a tool material) [2]. The cubic phase has been predicted to be the thermodynamically most stable structure of BN, but amorphous BN is generally obtained along with turbostratic modifications (t-BN) under typical laboratory synthetic conditions [6, 7]. Synthesis of c-BN has mainly been performed under high-temperature/high-pressure conditions. However, thin films of c-BN have recently been grown epitaxially on diamond by low pressure ion-beam-assisted CVD [8].

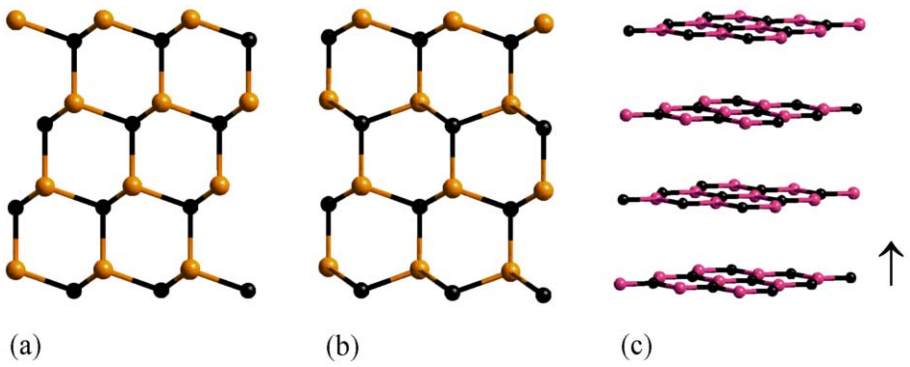

Figure 1.1: Models of (a) 3C-SiC or c-BN, (b) 2H-SiC and (c) h-BN. The arrow points in the [0001] and [111] directions of the hexagonal and cubic phases, respectively.

1.3 Structure

Silicon carbide possess several chemical structures, so-called polytypes, which can be considered as stacking variants of the Si-C double layers [1]. The 3C-SiC (zinc blende) and 2H-SiC (wurtzite) modifications have pure cubic and hexagonal stackings, respectively, in the hexagonal [0001]-direction (which corresponds to the cubic [111]-direction), see Fig. 1.1(a-b). Four indices are often used to characterize atomic planes for hexagonal systems. However,

one of the indices is redundant. For example, the hexagonal (0001) and (001) planes are equivalent [9]. However, (0001) is for conventional reasons used for hexagonal SiC throughout this work. The remaining hexagonal polytypes represent combinations of these stacking sequences. 4H-SiC has a stacking sequence of 4 Si-C bilayers and a c-axis of 10.1 Å which is to be compared with a c-axis of 5.2 Å for 2H-SiC. In all of these structures, the atoms are sp^3-bonded and every Si(C)-atom is tetrahedrally surrounded by four C(Si)-atoms (Fig. 1.2(a)). Cubic silicon carbide is also referred to as β-SiC, while all the hexagonal polytypes (2H-, 4H-, 6H-SiC etc.) are collectively referred to as α-SiC.

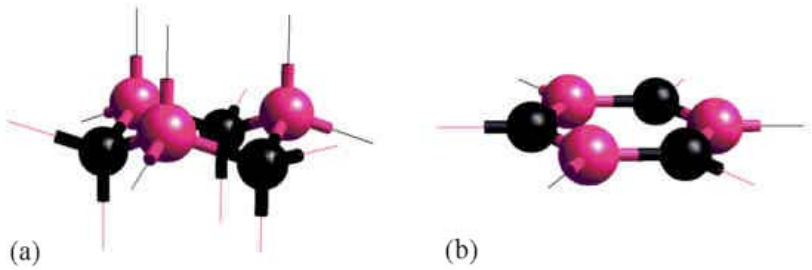

Figure 1.2: An illustration of the different geometrical surroundings of (a) sp^3-hybridized c-BN and (b) sp^2-hybridized h-BN.

Cubic boron nitride has zink blende structure. On the contrary, the hexagonal polymorph has a layered structure (with sp^2-hybridized B and N atoms) similar to graphite (Figs 1.1(c), 1.2(b)). The c-axis of h-BN is 6.66 Å, which is twice the inter-layer spacing between two successive sheets. The covalent bonds within the hexagonal layers are strong, while the intra-planar van der Waals interactions are very weak. Furthermore, the difference between t-BN and h-BN is that the hexagonal sheets are less ordered in the turbostratic modification, something which induces longer inter-layer distances [10].

Thin film growth

2.1 General

There are different ways to produce new materials. The starting materials can be in solid, liquid or gaseous form, and they can be combined and prepared in various ways. In physical vapor deposition (PVD), the solid precursors are sublimed by ion bombardment and subsequently deposited by condensation on a substrate. In chemical vapor (CVD) deposition, thin films are instead grown by chemical reactions of gaseous precursors on a substrate surface.

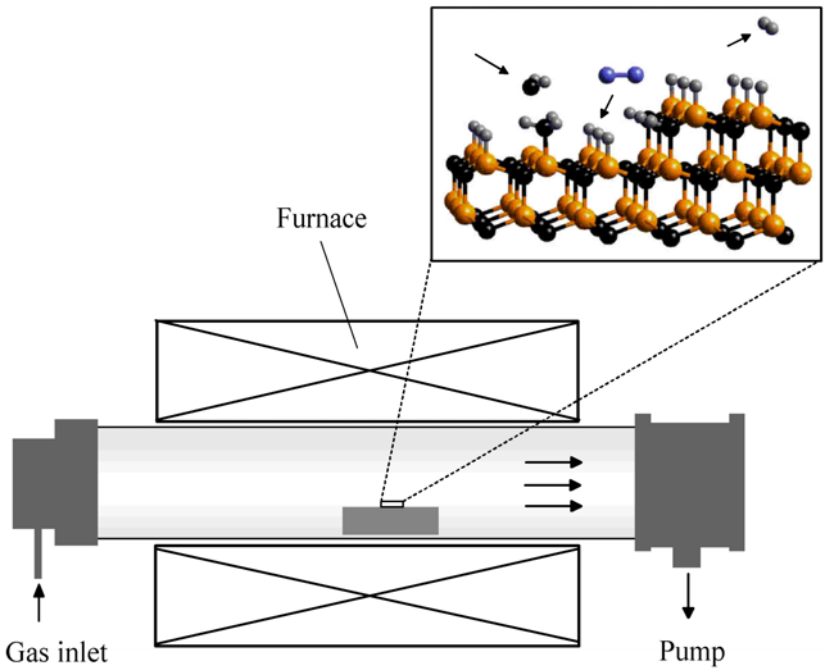

Figure 2.1: A hot-wall CVD reactor. The inset picture is a magnification of a growing SiC(0001) surface.

2.2 Chemical Vapor Deposition

2.2.1 Introduction

Thin films are in CVD grown by chemical reactions of gaseous precursors on, or in the vicinity of, a growing surface (Fig. 2.1). Materials with different properties can then be deposited by varying the experimental conditions (e.g., temperature, pressure, substrate material, gaseous composition, gas flow). In order to fully control the deposition it is important to understand the sequence of phenomena from where a gaseous species is generated, then reacts and finally becomes incorporated into the growing film. However, these processes are very complicated and only a few reaction mechanisms are known in detail.

2.2.2 Growth processes

During CVD, gaseous species adsorb to the growing surface, particles desorb (or become abstracted), they migrate and react with other species on the surface. New formations and bonds are then created. These type of elementary processes can, with advantage, be studied theoretically.

A gaseous species (A) can become adsorbed to a surface ($Surf\cdot$) according to:

$$Surf\cdot + A(g) \rightarrow Surf - A \tag{2.1}$$

The adsorption energies are then calculated using the following equation:

$$\Delta E_{ads}[A] = E[A] + E[Surf\cdot] - E[Surf - A] \tag{2.2}$$

where $E[Surf - A]$ and $E[Surf\cdot]$ are the total energies of the surface with or without an adsorbate, respectively. When the binding between the adsorbate and the surface is a weak interaction (of van der Waals type, i.e., $\Delta E_{ads}[A] \lesssim 35$ kJ/mol), the adsorption reaction is called physisorption. If a stronger (covalent, ionic or metallic) bond is formed, the adsorption reaction is instead referred to as chemisorption.

The desorption process of an adsorbed species from the surface can be regarded as reversed to the adsorption reaction (Eq. 2.1). Alternatively, surface-bonded species (A) are removed by abstraction reactions involving gaseous species (B). The Eley-Rideal (ER) abstraction mechanism is described by:

$$Surf - A + B(g) \rightarrow Surf\cdot + AB(g) \tag{2.3}$$

The main driving force of a chemical reaction can be obtained from thermodynamics. An endothermic reaction will not take place. However, an exothermic reaction is not certain to take place. For example, an exothermic adsorption reaction might be unfavorable because of a large adsorption barrier. Energy barriers for various surface reactions are, hence, important to take into account when studying growth mechanisms.

2.2.3 Precursors

Carbon- and silicon-containing gaseous species are deposited onto the growing surface during vapor growth processes of SiC. Silane (SiH_4) is the most common Si source, and a hydrocarbon (e.g., CH_4, C_2H_4 or C_3H_8) is often used as a C-supplying species [11]. Methyltrichlorosilane is a currently used single-source precursor. Moreover, the precursors are generally introduced in a large excess of H_2, which has the function of a carrier and co-reactant gas.

CVD-processes are generally controlled by mass transport phenomena and chemical kinetics. Only for very extreme experimental conditions (e.g., very low flow rates, high temperatures) a CVD process is actually controlled by thermodynamics. Nevertheless, thermodynamic calculations can give guidance also for non-equilibrium conditions. Many different gaseous species are formed upon thermal decomposition of the precursor gas in a CVD reactor [12]. The gaseous composition (suggested by thermodynamical calculations) can then be of help when choosing between plausible precursors for thin film growth (Paper **VI**).

Various B-containing precursors have been used for CVD of boron nitride (e.g., B_2H_6, BF_3, BCl_3, BBr_3, $B_3N_3H_6$ and $B_3N_3H_3Cl_3$) [13]. Ammonia is, because of its higher reactivity compared to N_2, the most commonly used N-supplying precursor. The NH_3 and BBr_3 precursors were used for the theoretical and experimental studies of BN growth included in the present thesis (Papers **IV** and **V**).

The precursors are usually thermally activated in CVD, and temperature is, hence, an important process parameter. The precursor molecules can also be activated by means of a hot-filament, UV light (photolysis) or the formation of a plasma etc. In Paper **V**, the NH_3 and BBr_3 precursors were either thermally and/or photolytically dissociated during the BN deposition experiments.

2.2.4 Substrate

Monocrystalline silicon has been widely used for CVD of SiC [11]. However, epitaxial growth of SiC is, with the availability of high-quality wafers, mainly performed on 4H- and 6H-SiC substrates [14]. The structure of the growing surfaces are important for growth, and this topic will be further discussed in Sec. 2.4.

The best candidate as a substrate for c-BN heteroepitaxial growth should be diamond since the two materials have closely related structures and unit cell parameters. Not until very recently, epitaxial films of c-BN have been successfully grown on diamond under low-pressure conditions [8]. Many different substrate materials other than diamond have been used for BN deposition (e.g., metals, ceramics, and glasses) [15, 4]. Cubic BN has also been found to nucleate on hexagonal boron nitride [16, 17]. SiO_2 and $\alpha - Al_2O_3(102)$ were used as substrates for the deposition of BN thin films presented in Paper **V**.

2.3 Atomic Layer Deposition

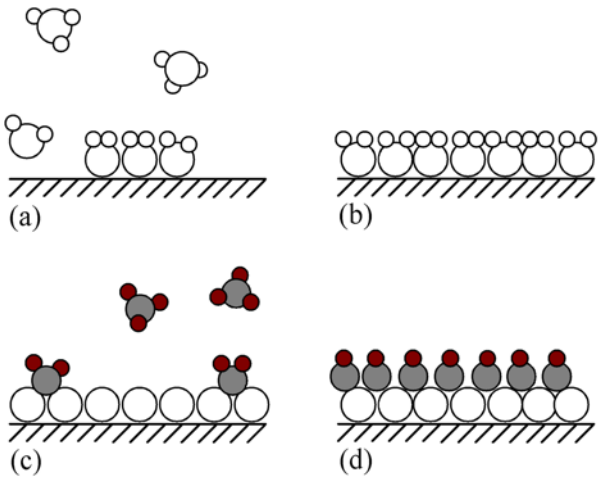

Figure 2.2: A schematic illustration of a four step ALD sequence. (a) Chemisorption of the first precursor gas. (b) Purging with an inert gas to remove excess precursor and reaction products. (c) Surface reaction with the second precursor gas. (d) Inert gas purging.

Atomic layer deposition (ALD) is a specific type of CVD, and the general concepts are similar for the two processes [18]. One major difference is that the precursor gases are separately pulsed into the reactor in ALD. Gas phase reactions between different precursors are then avoided, and the process is controlled by surface reactions. The different reaction steps in a four-step ALD sequence, as the one applied in Paper **V**, are described by Fig. 2.2. In the ALD process, the thickness is governed by the number of cycles instead of the deposition time (which is the situation in an ordinary CVD process). An excellent step coverage and thickness control is generally obtained. Hence, a

well-functioning ALD process can be controlled at an atomic level.

2.4 Surfaces

2.4.1 General

A non-polar surface of an insulating, cubic material (e.g., sodium chloride) may exhibit a structure which is close to the ideal bulk structure. However, an altered surface structure is generally obtained upon cleavage of a material. The reason for this is that the atoms on a surface of a material are not completely surrounded by atomic neighbors. In bulk zink blende, every atom binds tetrahedrally to four neighboring atoms. However, on the surface of c-BN(111) or β-SiC(111) $\big($being equivalent to α-SiC(0001)$\big)$, one covalent bond per atom is broken upon cleavage. As a result, each surface atom has one dangling bond (containing an unpaired electron). The surface energy is higher for more open surfaces, with higher concentrations of dangling bonds. The (111) $\big($or (0001)$\big)$ surface is the relatively most stable of the SiC surfaces, and it is generally believed to be the main growth direction [1]. Moreover, adsorption of precursor species is more favorable at steps than on flat surfaces. An off-axis of a SiC(0001) substrate is often used. (A typical off-axis for 6H-SiC of 3.5° corresponds to a surface step every 15^{th} unit cell.)

Growth of c-BN has been predicted to occur by the (111) or (001) planes [19, 20, 8]. For the h-BN polymorph, (001) is likely to be the main growth direction [21]. The c-BN(111), β-SiC(111) and α-SiC(0001) surface planes are polar since each of them exclusively consists of one type of atoms [1]. In the present work, both planes have been included when studying any of these surfaces (Papers **I**, **II**, **IV** and **VI**).

2.4.2 Reconstructions

Surface atoms are more loosely bound compared to atoms in the interior of a material. The reason is that they do not have a bulk-like environment. However, they strive to lower the surface energy, and this results in various surface structures; (i) the surface atoms relax, (ii) they become reconstructed, (iii) islands form on the surface. Experimental and theoretical investigations of the Si-surface of hexagonal SiC(0001) have among others shown the (1x1), $(\sqrt{3}x\sqrt{3}) - \text{R}30^\circ$, (3x3) or the $(6\sqrt{3}x6\sqrt{3}) - \text{R}30^\circ$ reconstructions [22, 23]. The corresponding C faces have shown the (1x1), (2x2), (3x3), or $(\sqrt{3}x\sqrt{3}) - \text{R}30^\circ$ reconstruction [22, 23]. Moreover, for one specific surface reconstruction, different downward relaxations have also been observed. The surface structures of c-BN are not as extensively studied. Nevertheless, for the c-BN(111) and c-BN(100) surfaces, a number of reconstructions $\big($including (1x1),

(2x1), (2x2) and(2x4)) have been examined theoretically [24, 25]. In the present work, unterminated 4H-SiC(0001) surfaces have been studied (Paper **I**).

2.4.3 Terminations

Silicon carbide samples prepared by oxidation and HF treatment exhibit unreconstructed (1x1) SiC(0001) surfaces, where the surface dangling bonds are saturated by terminating adatoms such as oxygen, hydrogen or hydroxyl species [23]. Further treatment in hydrogen plasma has been found to induce H-(1x1) structures [21, 26]. The presence of gaseous hydrogen molecules and radicals during SiC growth is then supposed to sustain the sp^3-hybridization of the surface (Si or C) atoms.

The hydrogen atom has theoretically been predicted to be a good terminating species also for the c-BN(111) surface [27]. Specifically, hydrogen was found to (i) maintain the sp^3-hybridization of the surface B (N) atoms and (ii) become abstracted from the growing surface, and thereby make room for a precursor growth species. Furthermore, fluorine has been found to bind very strongly to the c-BN(111) surface [27, 20]. Powerful energetic activation, such as energetic ion bombardment, seems to be necessary in order for surface-bound fluorine atoms to desorb. Hydrogen-termination of the surfaces was applied in the theoretical investigation of SiC and BN growth which is presented in Papers **II**, **III**, **IV** and **VI**.

Computational methods

3.1 General

Many people think that chemistry is all about boiling pink liquids in spherical containers. However, in theoretical chemistry, quantum mechanics is used to compute the properties of molecules and their interaction with each other. The ground state geometrical structures and energies of molecules can, for example, be calculated theoretically given a set of nuclei and electrons. A large number of molecular properties (e.g., dipole moment, vibrational spectra) can also be obtained. Depending on the accuracy of the theoretical method, systems containing hundred to thousand particles can be studied.

3.2 Quantum mechanical calculations

In order to describe the detailed electronic structure of a molecular system, *ab initio* quantum mechanics must be used. Basically, one has to solve the time-independent Schrödinger equation, which can be written as:

$$\hat{H}\Psi = E\Psi \tag{3.1}$$

where E is the electronic energy, Ψ is the wavefunction, and $\hat{H}$ is the Hamiltonian operator. $\hat{H}$ consists of terms describing the kinetic energy ($\hat{T}$), the electron nucleus attraction energy ($\hat{V}_{ne}$), and the electron electron repulsion energy ($\hat{V}_{ee}$).

$$\hat{H} = \hat{T} + \hat{V}_{ne} + \hat{V}_{ee} \tag{3.2}$$

By determining the eigenfunctions (ψ_i) with corresponding eigenvalues (E_i), all properties of the system can be obtained. Unfortunately, no strategy to solve the Schrödinger equation exactly for many electron systems is known, and various approximations must be used. The Born-Oppenheimer approximation is usually applied for chemical problems. It states, due to the mass difference between the atoms and electrons, that the electronic and nuclear motions, can be treated separately. The parameters involved are, in many types of theoretical methods, obtained by fitting to experiments. However, in *ab initio* techniques,

solutions to the Schrödinger equation are generated without reference to experimental data. This can, for practical reasons, only be done for systems smaller than a few hundred atoms. The two main *ab initio* schemes for solving Eq. 3.1 are Hartree-Fock (HF) and Density Functional Theory (DFT).

3.2.1 Hartree-Fock theory

Hartree-Fock methods are based on different descriptions of the wave function in the Schrödinger equation. In this scheme, the wave function, ψ_i, is approximated by using a linear combination of atomic orbitals (LCAO). The resulting wave-function is often referred to as the Slater determinant,

$$\Psi_{HF} = \frac{1}{\sqrt{N!}}\det[\psi_1\psi_2...\psi_N] \tag{3.3}$$

Ψ_{HF} is an antisymmetric product of N one-electron wave functions (ψ_i). Each one-electron function is composed of a spatial atomic orbital and a spin function. In HF methods, the exact solution of Eq. 3.1 is systematically approached by a series of increasingly refined approximations of ψ_i. According to the variational principle, the energy computed by a trial wave function will be an upper bound to the true energy of the ground state. The energy of the system can be expressed as:

$$E_{HF} = \sum_{i=1}^{N} H_i + \frac{1}{2}\sum_{i,j=1}^{N}(J_{ij} - K_{ij}) \tag{3.4}$$

where H_i comprises the kinetic energy as well as the electron nucleus attraction, and J_{ij} and K_{ij} are the Coulomb and exchange integrals, respectively. The difference between the HF energy and the exact energy of the system depends mainly of the correlation between the electronic motions. Different methods are, hence, used in order to account for the correlation energy. The second order Møller-Plesset (MP2) perturbation theory was used to account for the electron correlation by perturbing the HF solution in Paper **III** [28]. Refined methods such as MP2 give more accurate results but they are also very time-consuming.

3.2.2 Density Functional Theory

The basic idea behind DFT is that the energy of an electronic system can be written in terms of the electron density, $\rho(\mathbf{r})$ [29, 30]. $\rho(\mathbf{r})$ determines the probability of finding any of the N electrons in a system within the volume d$\mathbf{r}$.

$$\int \rho(\mathbf{r})\mathrm{d}\mathbf{r} = N \tag{3.5}$$

The energy, E, is a functional of the electron density, and for a given function $\rho(\mathbf{r})$ there is a single corresponding electronic energy, $E[\rho]$. In DFT, functionals connecting the electron density with the energy of the system have to be designed. Kohn and Sham suggested that the energy of a system only depends on the electron density [31]. The ground-state energy of a system can then be written as:

$$E[\rho] = T[\rho] + E_{ne}[\rho] + J[\rho] + E_{xc}[\rho] \tag{3.6}$$

The challenge is to find a proper description of the exchange-correlation energy, E_{xc}. In the Local Density Approximation (LDA), it is expressed as

$$E_{xc}[\rho] = \int \rho(\mathbf{r})\varepsilon_{xc}\left[\rho(\mathbf{r})\right] d\mathbf{r} \tag{3.7}$$

where $\varepsilon_{xc}\left[\rho(\mathbf{r})\right]$ is the exchange-correlation per electron in a homogeneous electron gas. LDA generally gives good geometries, but it does not treat bonding energies in an acceptable way. A way to improve the LDA approach is to make the exchange and correlation energies dependent not only on the electron density $\rho(\mathbf{r})$, but also on derivatives of the density, $\nabla\rho(\mathbf{r})$. Such methods are known as Generalized Gradient Approximation (GGA) methods, and they usually give improved results compared to LDA.

DFT was applied in Papers **I**, **II**, **IV** and **VI**. A LDA functional developed by Perdew and Zunger, as well as a GGA method developed by Perdew and Wang, were then used [32, 33]. The electron density is more easy to work with than the complicated wave function in the Schrödinger equation and it can, hence, be applied for fairly large systems. Since it is valid for all elements in the periodic table, DFT has become widely used in chemistry and physics.

3.3 Basis sets

The atomic orbitals are generally described by analytical basis sets within the Hartree-Fock method. In MO-LCAO, the molecular orbitals, ψ_i, are composed of linear combinations of one-electron basis functions, χ_i, according to:

$$\psi_\mathrm{i} = \sum_{\mathrm{j}=1}^{N} c_{\mathrm{ij}}\chi_\mathrm{j} \tag{3.8}$$

These functions are in turn formed by linear combinations of primitive Gaussian functions, g_k:

$$\chi_j = \sum_k d_{jk} g_k \tag{3.9}$$

The coefficients in the contracted functions are not independently varied in the SCF procedure. A basis set consisting of many atomic functions will give a more flexible total wave function, which better describes the electronic structure of the system. The 6-31G** split-valence basis set with polarizing functions was used in Paper **III**.

A system can be represented by a super-cell with periodic boundary conditions. For a periodic system, the electronic wave functions can, according to Bloch's teorem, be expanded in plane waves [34].

$$\psi_{\mathbf{k}}(\mathbf{r}) = \sum_{\mathbf{G}} C_{\mathbf{k}\text{-}\mathbf{G}} e^{i(\mathbf{k}-\mathbf{G})\cdot\mathbf{r}} \tag{3.10}$$

where **G** is the reciprocal-lattice vector and C represents the wave function expansion coefficients. The energy of a system can then be calculated for a set of **k**-points. The Monkhorst-Pack scheme was used to generate an adequate number of **k**-points in Papers **I**, **II**, **IV** and **VI** [35]. Generally, a very large basis set is required to perform an all-electron calculation. In the pseudopotential approximation, the core electrons and ionic potential are replaced by a weaker pseudopotential. The electronic wave functions can then be expanded using a much smaller number of plane waves. The pseoudopotential is angular-momentum dependent, or nonlocal. Nonlocal pseudopotentials in the Kleinman-Bylander separable form were used for the DFT calculations presented in Papers **I**, **II**, **IV** and **VI** [36]. The plane-wave basis sets were truncated to include plane waves with kinetic energies less than a specified cutoff energy.

Two electrons with different spins share one spatial orbital in restricted calculations, and this is often sufficient for close-shell systems (containing an even number of electrons). For systems containing an odd number of electrons, unrestricted calculations in which each electron is related to a unique effective potential are generally preferable.

3.4 Geometry optimization

A solid adopts the structure that minimizes its total energy. A stable structure or, computationally seen, a zero-slope energy derivative point can often be found quite easily and accurately by using standard algorithms for finding

extrema on a multidimensional surface. However, these calculations are only approximations to the real system, and there is always a possibility that the optimization procedure will end up in a transition state. Various degrees of freedom, including internal coordinates and cell parameters, are then considered. Partial geometry optimization of a system can be performed by freezing one or more of the atomic positions and/or cell parameters. As an example, the closest atomic neighbors of an adsorbate-bonding surface atom can be relaxed during a geometry optimization, while the remaining atoms in the surface model are fixed. The characteristics of a more realistic surface than the one explicitly modelled can in this way be obtained. The conjugate gradient BFGS procedure was used for geometry optimization calculations in Papers **I**, **II**, **IV** and **VI** [37]. The Berny algoritm was used in the HF calculations (Paper **III**).

3.5 Dynamics

DFT is a zero-temperature method in the standard formulation. However, it is possible to perform *ab initio* dynamic calculations (based on DFT) for finite temperatures. To generate correct dynamical trajectories, the electrons must be relaxed to the ground state at each time step. It is then possible to simulate the motions of the atomic nuclei as they will occur in a chemical reaction. A typical step time is 10^{-15} s, and a simulation, hence, tends to sample only the region in phase space close to the starting conditions.

In Paper **II**, an approach was applied where the nuclear motions were treated by solving the Newtonian equations using the Verlet velocity propagator [38, 39]. The nuclear forces that determine the acceleration of the atoms were obtained using DFT calculations. The canonical ensemble (NVT) was obtained by controlling the thermodynamic temperature applying the Nosé thermostat [40].

3.6 Model accuracy

In order to adequately describe the electronic structure of a system it is important to use an appropriate model. Surfaces can be represented either by discrete cluster models or by supercells consisting of two-dimensional slabs. Both approaches have been applied in the present thesis. For every surface model it is important to use:

1. A flexible enough basis set.

2. A large enough surface model. When modelling cluster surfaces, the atoms terminating the template must attempt to simulate a continuation of a real cluster. In supercells, the atomic layers must be thick enough

and the vacuum size must be wide enough to avoid interactions between two surfaces.

3. A suitable number of geometry optimized surface atoms.

Experimental methods

4.1 The ALD reactor

In a hot-wall ALD (or CVD) system, energy is generally supplied to the precursor molecules by heating. In order to further enhance the reactivity of precursors, photochemical activation was also applied in Paper **V**. An ArF excimer laser, operating at 193 nm, was then applied. The experiments were carried out in a specially designed horizontal hot-wall ALD-reactor (Fig. 4.1). N_2 was used for purging and as as carrier gas for the gaseous NH_3 and BBr_3 precursors. The BN films were deposited on single-crystalline $\alpha - Al_2O_3(102)$ and SiO_2 substrates in the temperature range 250-750 °C.

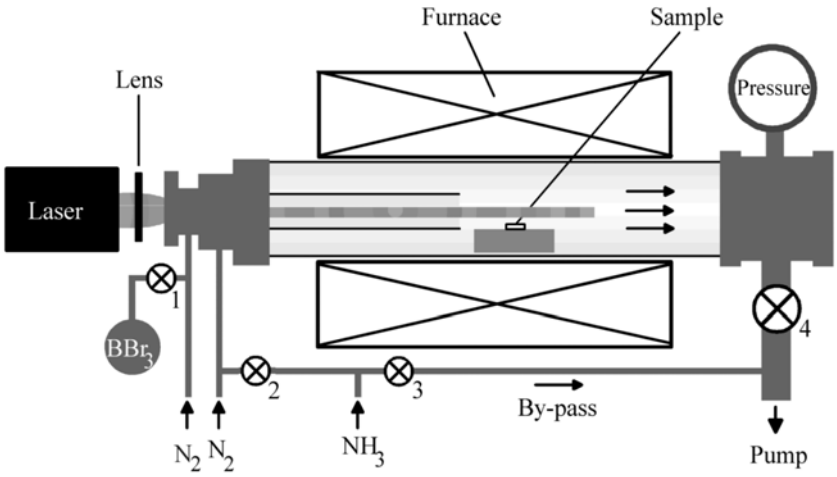

Pulsing scheme	NH_3	Purging	BBr_3	Purging
Valves open	2	3	1,3	3
Valves closed	1,3	1,2	2	1,2

Figure 4.1: Schematic drawing of the reactor and a table describing which valves were open for the different gas pulses in an ALD cycle. A needle valve (4) was used to keep a constant pressure in the reaction chamber.

4.2 Characterization

In order to be able to optimize a growth procedure, it is necessary to characterize the deposited material in an appropriate way. The chemical composition and structure of the sample are generally important to find. However, many other properties (such as hardness, thermal conductivity etc.) might also be of interest.

Boron and nitrogen are very light elements and it is, hence, difficult to obtain diffraction patterns from thin BN films. Especially when they are not well-crystallized. For low incidence angles, information about the outermost layers (typically 5-10 nm for $\phi < \phi_c$) can be obtained for planar surfaces by X-ray Diffraction (XRD) (Fig. 4.2). The Grazing Incidence (GI) XRD method was, hence, used to enhance the signal from the surface when determining the structure of the deposited BN material. X-Ray Reflectivity (XRR) was used to measure the density, thickness and surface roughness (Fig. 4.2). Furthermore, the composition was studied by X-ray Photoelectron Spectroscopy (XPS). Fourier Transform Infrared (FTIR) spectroscopy (transmission mode) was performed in order to estimate the relative H-concentration.

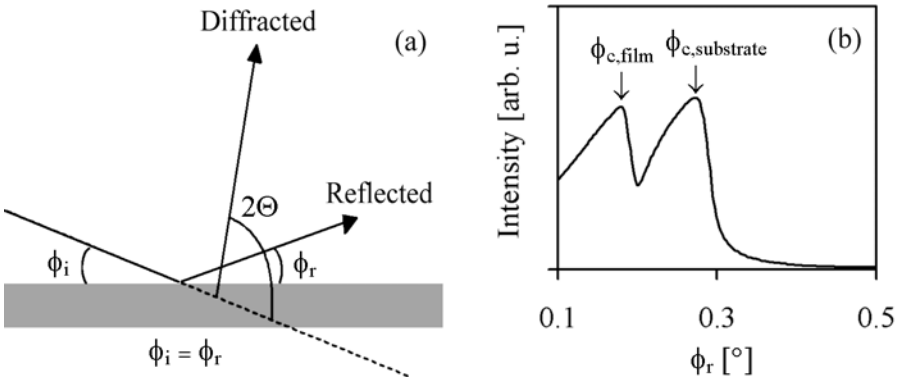

Figure 4.2: (a) In GI-XRD measurements, the incidence angle, ϕ_i, is locked as the detector is swept through a desired 2Θ region. Moreover, total reflection of X-rays can be obtained for low incidence angles. At the critical angle, ϕ_c, the reflected intensity reaches half the value observed in the total reflection region. The material density can be deduced from ϕ_c. (b) Total reflection for a BN film deposited on $\alpha - Al_2O_3(102)$. (ρ_{BN} = 1.8 g/cm^3 and $\rho_{Al_2O_3}$ = 4.0 g/cm^3.)

Results

5.1 General

This part of the thesis presents the major results of the included articles. The results are divided into studies of (i) surfaces, (ii) growth processes, and (iii) incorporation of dopant and contaminant species.

5.2 Unterminated 4H-SiC(0001) surfaces

SiC surfaces adopt various reconstruction structures. Experimentally determined surface reconstructions are generally used for theoretical investigations of α-SiC(0001) surfaces [22]. It has also been common to allow downward relaxation of a model with a fixed structure in the x- and y- directions. Surface reconstructions of unterminated 4H-SiC(0001) surfaces were in Paper **I** investigated by using DFT. The reconstructed surface was then obtained theoretically starting from a 4H-SiC(0001) surface model with an ideal bulk geometry. The uppermost four atomic layers of the model were allowed to relax in three dimensions during the geometry optimization calculations.

As a result, the displacement of the atoms was, for both surfaces, small in the x- and y- directions. For the Si-rich surface model, the distance between the first and second atomic layers decreased (in average by 21 %) compared to the initial bulk positions. This is in general agreement with earlier theoretically obtained results [22]. Moreover, the surface exhibited a buckled (2x1) reconstruction in the c-direction, such that half of the surface Si atoms formed a novel surface layer while the rest formed a second layer underneath (Fig. 5.1). Furthermore, the C(0001) surface retained its initial (1x1) structure through the geometry optimization calculations. The downward relaxation was, on the other hand, much larger (i.e., about 45 %) for the C surface than for the Si surface.

A (2x1) reconstruction pattern of the SiC(0001) surface has, to the knowledge of the present author, not been observed experimentally [23]. However, buckling reconstructions (not being changed in the x- or y- directions) can be experimentally difficult to differ from (1x1) surfaces, and the occurrence of (1x1) patterns is well-established [41, 23].

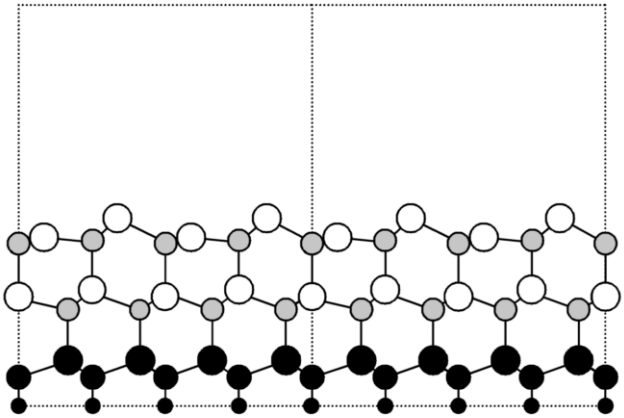

Figure 5.1: Side view of the geometry-optimized 4H-SiC(0001) model, in which every second Si-atom of the top layer is raised above the other ones, causing a (2x1) reconstruction of the surface.

5.3 Growth at the atomic level

5.3.1 4H-SiC(0001) surfaces: Adsorption

Gaseous C_2H_2 and Si species are assumed to be important as carbon- and silicon-containing growth species during CVD of SiC [12]. The effects of C_2H_2 (or Si) adsorption on the two reconstructed 4H-SiC(0001) surfaces, described in the previous section, were also studied in Paper **I**. The adsorption reactions were then assumed to occur according to Eq. 2.1. As a result, both adsorption reactions were structurally found to influence the surface geometries in the direction of bulk parameters. The energy for adsorption of C_2H_2 to the Si plane was found to be 675 kJ/mol (for 2-fold adsorption) and the corresponding energy for Si adsorption to a 3-fold hollow site on the C plane was 880 kJ/mol on the GGA level of theory. The two-fold C_2H_2 and one-fold Si adsorption energies have earlier been estimated to 410 and 368 kJ/mol, respectively, for unterminated 3C-SiC(111) surfaces at 298 K by using the Langmuir model [42]. For Si adsorption, the discrepancy can mainly be explained by the different binding situation. Moreover, the difference in computational models, as well as the two temperatures applied, are other important reasons for the numerical difference observed.

5.3.2 4H-SiC(0001) surfaces: Abstraction

Hydrogen is assumed to be capable of forming single bonds to the surface atoms in SiC, and thereby sustaining the sp^3-hybridization [21, 23, 43, 44, 26]. However, the presence of gaseous H atoms in the atmosphere above the growing surface can both facilitate surface-termination and remove surface-binding H atoms via abstraction reactions (Eq.2.3). It is not certain that H atoms will be chemically bonded to a SiC surface at normal experimental vapor deposition temperatures.

The main idea of Paper **II** was to energetically investigate the formation of unterminated areas on the 4H-SiC(0001) surface. Hydrogen abstraction by gaseous X radicals (X = H, F, Cl, Br) from H-terminated 4H-SiC(0001) surfaces was then theoretically investigated. The calculations were performed by means of *ab initio* molecular dynamics. Both the Si and C planes were investigated at the temperatures 1600 and 2300 °C. The abstraction of a binding H atom from a completely H terminated surface, as well as the abstraction of a second H bonded to a surface atom adjacent to the initially created surface radical, were then investigated. Moreover, the H adsorption reactions for each of the resulting mono- or diradical sites were also included in this study.

The H abstraction reactions were found to be only slightly exothermic or endothermic. Hydrogen abstraction by a halogen radical was in all cases found to be more favorable than abstraction by a H radical, with the following order of energies H $<$ Br $<$ Cl $<$ F. However, H adsorption was found to be more favorable than the corresponding abstraction reaction. The abstraction reactions were generally found to be more exothermic (or less endothermic) for the Si surface than for the corresponding C surface. In summary, the present results imply that H-termination of SiC(0001) surfaces (especially then the C surface) is energetically stable enough to endure temperatures as high as 2300 °C even in the presence of gaseous hydrogen or halogen radicals.

5.3.3 β-SiC clusters

Clusters of various sizes and shapes may be obtained homogenously in the gas phase during CVD. They are also expected to occur on the growing surface, either by adsorption of a gaseous cluster or as a local formation
created on the surface during growth. These cluster-like particles include various numbers of atoms. The properties of these clusters generally differ from those of bulk materials [45]. The growth of β-SiC clusters from gaseous precursors CX_3 (X=H, F) has been theoretically studied in Paper **III**. Gaseous C_2H_2, has been predicted to be the major C-contributing species during vapor growth of SiC, but other species (e.g., CX_3) are probably also important under certain experimental conditions [42, 46]. Experimental temperatures that are used during deposition are expected to influence the processes occurring on a

growing surface. However, if the numerical difference between two energies (e.g., two adsorption energies) is $\geqslant 1$ eV at 0 K, their relative order is generally expected be maintained for increased temperatures.

The purpose of the work presented in Paper **III** was to make a comparative structural and energetic investigation considering the adsorption of various species to β-SiC clusters of various shapes and sizes. The species included were H and CH_3, or in some cases F and CF_3, and the study was carried out by using *ab initio* MO theory. Four different clusters were included; the roundish clusters I and IV, as well as the planar clusters II and III, which can be regarded to model small parts of the (111) and (100) surfaces, respectively (Fig. 5.2).

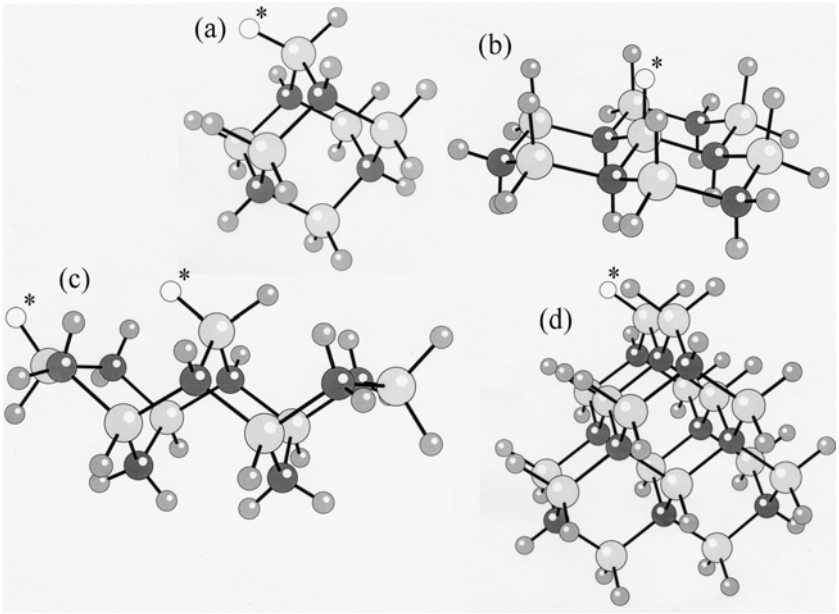

Figure 5.2: Models of cluster (a) I ($Si_6C_4H_{16}$), (b) II ($Si_7C_6H_{21}$), (c) III ($Si_7C_8H_{23}$), and (d) IV ($Si_{16}C_{10}H_{32}$). The adsorption sites are marked with a "*".

The H adsorption energy was found to be significantly larger for the smaller cluster I (484 kJ/mol) than for the larger cluster IV (369 kJ/mol). This implies that the cluster size does affect the adsorption process and that self-termination of the cluster growth may occur at larger sizes. Moreover, the possibility for CH_3 to replace a surface-terminating H species on the surface of a SiC cluster is a measure of how suitable the combination H/CH_3 is for C growth on this specific material. The energy difference between adsorption of CH_3 and H $\left(\Delta E_{ads}(\mathrm{CH_3}) - \Delta E_{ads}(\mathrm{H})\right)$ was found to be within the range -94 to 55 kJ/mol.

(As stated in Eq. 2.2, exothermic and endothermic reactions corresponded to positive and negative adsorption energies, respectively.) This means that CH_3 and H form bonds that do not differ appreciably in strength (for all the investigated clusters). Moreover, the effect of different terminating species X (X = H, F) was also investigated by performing a corresponding adsorption study using F and CF_3 in addition to H and CH_3. The F adsorption reaction to a F-terminated cluster I was then found to be significantly more exothermic (by 324 kJ/mol) than the corresponding CF_3 adsorption reaction. The general trend obtained for CF_3 and F adsorption indicated that the presence of fluorine would not favor a continued growth of SiC clusters.

The following conclusions could be drawn from the study; (i) the initial stage of C growth on Si surface sites of SiC clusters are energetically more favorable using H, instead of F, as the terminating species, (ii) the corresponding adsorption processes were also (from a geometrical point of view) markedly ideal for small, roundish clusters instead of more planar ones. Hence, a rough SiC surface, consisting of a large number of small and more roundish cluster-like SiC particles, seems to be more favorable for growth than a smooth and mainly planar SiC surface.

5.3.4 c-BN(111) surfaces

Both F and H have by Larsson been found to sustain the the structure of cubic boron nitride surfaces [27]. Hydrogen was then theoretically predicted to be a favorable surface-terminating species for c-BN growth by ”gentle” chemical vapor methods. On the contrary, the F-stabilized c-BN(111) surface was found to be resistant to chemical abstraction and to prevent a continued growth by chemical means. (A continued c-BN growth of a F-terminated surface has instead been shown possible to occur by processes involving ion bombardment [20].) In the present work, the focus has been on growth via more gentle chemical reactions. The initial elementary reactions for vapor growth on H-terminated c-BN(111) surfaces was theoretically investigated in Paper **IV**. The adsorption of gaseous NH_3 and BBr_3, as well as their decomposed fragments, to c-BN(111) surfaces was then studied by using of DFT.

The considered adsorption reactions were with two exceptions, found to be exothermic. The endothermic reactions include adsorption of NH_3 and BBr_3 to the N-rich and B-rich surfaces of c-BN(111), respectively. The adsorption of N and NH was found to preferably result in the formation of N-N bonds in the growing film. Such bonds are not present in an ideal BN structure, where every N atom binds to four B atoms. NH_2 and NH_3 were, on the contrary, found to be favorable for ideal layer-by-layer growth of BN films. Moreover, gaseous B, BBr_2 and BBr_3 species were found to bind stronger to the N-rich compared to the B-rich surface of c-BN(111), while BBr was found to form similar bonds

two both surfaces. The N*-BBr_X bond, where the asterisk denotes an atom on the N-rich c-BN(111) surface, was found to decrease for X going from 0 to 3 (Fig. 5.3).

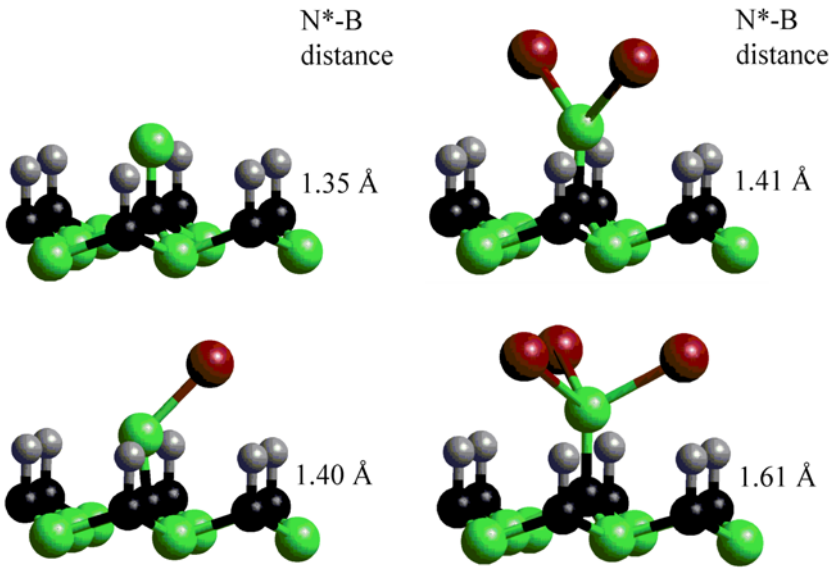

Figure 5.3: The binding situation of BBr_X (X=0-3) on the N*-rich surface of c-BN(111). The corresponding bond lengths between the surface N-atom and the B atom of the adsorbate, is placed next to each of the figures.

NH_3 and BBr_3 corresponded to the smallest adsorption energies of the precursor species included in this study. Nevertheless, they were predicted to constitute the most promising combination for ideal growth of c-BN(111) surfaces by vapor deposition involving mixed precursor gases. Gaseous N, NH and BBr species were on the other hand found to be unfavorable under such conditions. The reason was the risk of N-N and B-B bond formation. Furthermore, chemisorption of NH_2, B or BBr_2 were predicted to preferably form B-N bonds to c-BN(111), but to also with a certain possibility result in N-N or B-B bonds. When using these precursor species, there is, hence, a large probability to obtain a mixture of adsorbed B and N species on the (111) surface of c-BN. An ALD process, with separate precursor introduction, would prevent such a situation. The dissociation of the NH_3 and BBr_3 precursors would instead be favorable for an ideal ALD process.

5.3.5 ALD of BN thin films

BN thin films were in Paper **V** experimentally grown from NH_3 and BBr_3 precursors by using ALD and LALD (applying an ArF excimer laser). Atomic layer deposition of hexagonal BN films have earlier been reported twice, involving exclusively thermal heating of the precursors [47, 48]. By assuming an ideal ALD process, dissociation of NH_3 and BBr_3 would, due to the increased reactivity of the dissociated species, favor a continued c-BN growth (Sec. 5.3.4). Moreover, photochemical dissociation of NH_3 molecules would supply hydrogen radicals to the process. This would be advantageous since H atoms have been predicted to (i) stabilize cubic BN surfaces and (ii) make c-BN nucleation possible on various h-BN sites [27, 49, 16].

The ability of the ArF excimer laser to dissociate NH_3 and BBr_3 was confirmed by optical emission spectroscopy. During laser irradiation of NH_3, light emission from NH was detected in the gas phase while emission from B and BBr was observed during the BBr_3 gas sequence. Hence, NH_2, H, H_2, BBr_2, Br and Br_2 were assumed to also form.

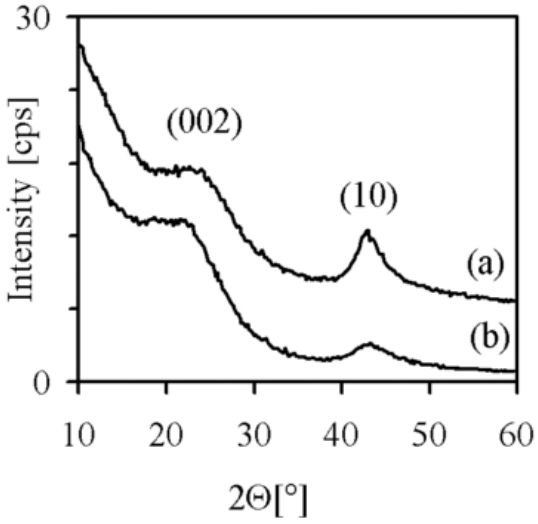

Figure 5.4: X-ray diffractograms, obtained for two BN films, deposited by (a) LALD and (b) ALD at 400 °C.

The structure of the deposited BN films was only found to be slightly improved as a result of LALD compared to ALD. By XRD, two diffuse diffraction peaks could be distinguished, namely (002) and (10) (Fig. 5.4). (The (10) peak is a mixture of the (101) and (100) peaks). The deposited films contained

predominantly t-BN with d_{002}-values of 7.1-7.9 Å, compared to 6.66 Å for h-BN. The lower d-values within the mentioned range were obtained for films deposited by LALD or by ALD at the higher of the temperatures applied (400-750 °C). However, the growth rate of the BN films increased by more than 100 % (from 0.45 - 1.2 Å/cycle) when using laser activation for deposition temperatures in the interval 250-600 °C (Fig. 5.5). This difference in growth rate was a result of photochemical dissociation of the BBr_3 precursor since photolysis of solely the NH_3 precursor gas did not alter the growth of the BN thin films.

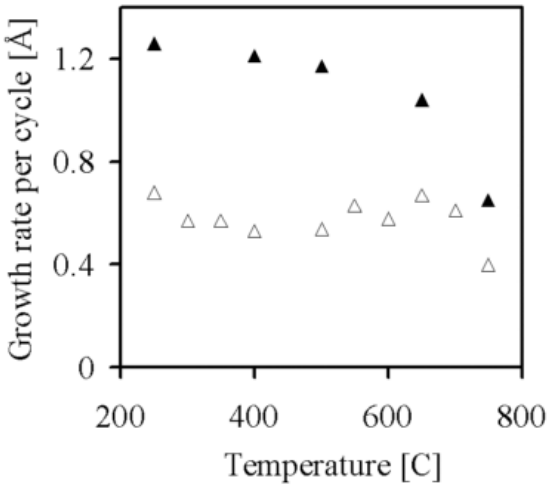

Figure 5.5: The influence of deposition temperature on the growth rate per cycle of the BN films obtained by ALD (△) and LALD (▲).

Similar BN material densities (i.e., 1.7-1.9 g/cm^3) were obtained for the different process temperatures applied (250-750 °C). However, the density of the BN films deposited below 600 °C by ALD decreased (to 1.5 - 1.7 g/cm^3) after a few days in atmosphere. The B/N composition ratio of the films was close to 1 and contaminant concentrations were low in the fresh samples. However, when exposed to air, the films were found to incorporate considerable amounts of oxygen and carbon. The films grown by LALD were then more stable against oxidation compared to the films grown by ALD.

Nanocrystalline BN grains, which were more extended in the intraplane (a-/b-) direction compared to in the interplanar (c-) direction, constituted the deposited films (Fig. 5.6). This probably accounts for the low densities obtained. The grains were larger in the films obtained by LALD compared to by ALD. Moreover, hydrogen atoms were (by FTIR) observed in the BN samples. The

relative H content was then found to be lower in the films deposited by LALD (compared to ALD). By assuming that the BN grains were H-terminated, the lower H-concentration in these films can be explained by the smaller percentage of surface sites available on larger compared to smaller grains (i.e., $\sim$12 and $\sim$21 atomic-%, respectively).

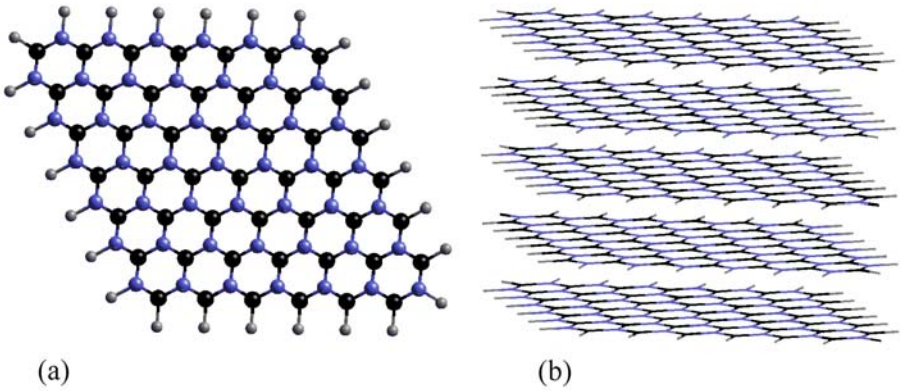

Figure 5.6: A plausible model of the nanosized grains, which constituted the BN films grown. (a) A top view of a $\sim$ 17 Å x 17 Å large BN sheet. (b) A side view of 5 H-terminated BN layers, corresponding to 13 Å in h-BN.

5.3.6 h-BN(001) edges

Generally, the hexagonal BN phase is to various extent present in thin films of c-BN [13]. An understanding of the adsorption processes during ”gentle” deposition of BN thin films, also involving this phase, would be of ultimate help in finding the prerequisites for ideal growth of c-BN. At the same time, it would then be possible to discriminate or favor h-BN growth. The theoretical investigation of c-BN growth, which has been described in Sec. 5.3.4, was for these reasons completed by also involving growth of h-BN (Paper **IV**). The adsorption processes of NH_X and BBr_X (X = 0-3) to hexagonal BN(001) edges was then studied.

The N-contributing precursors should have preferences for binding to B sites, and vice versa, in order for an ideal BN growth to occur. The adsorption of NH, NH_2, B and BBr was predicted to favor an ideal growth of h-BN. However, adsorption of NH_2 was favorable for both the hexagonal and cubic phases. On the contrary, the presence of N, BBr_2, and BBr_3 would preferably result in the formation of N-N or B-B bonds in the h-BN structure.

The BN films deposited in Paper **V** were found to include a considerable amount of hydrogen during growth. The hydrogen was then probably bound to edges of the hexagonal BN sheets (Fig. 5.6). The investigated BN growth species (i.e., BBr_X or NH_X, X = 0-3) were predicted to energetically have strong competition from H and H_2 when adsorbing to the B- and N-rich edges of the growing h-BN thin film. This is probably one reason for the formation of H-terminated nanocrystalline BN grains, instead of a continued growth of BN sheets (Fig. 5.6). Moreover, of the theoretically investigated precursor adsorption processes, only adsorption of a B radical to the N-edge of h-BN(100) was found to be energetically more favorable than the corresponding H adsorption reaction. The presence of B radicals in the gaseous atmosphere above the growing BN surface in Paper **V** is, hence, probably an important reason for the increased growth rate in LALD compared to ALD at intermediate temperatures.

5.4 Material modification

5.4.1 General

A material always contains impurities to different degrees. A cubic centimeter of SiC roughly consists of 10^{22} Si and C atoms and by using very sensitive characterization techniques it is possible to detect impurities at concentrations above $10^{11} - 10^{12}$ cm^{-3}. Doping of a material is either unintentional or intentional. Intentional doping can be accomplished by (i) diffusion into the material, (ii) ion implantation or (iii) *in situ* during growth.

5.4.2 N-incorporation into 4H-SiC(0001)

Unlike silicon, SiC cannot be efficiently doped by a diffusion process, and reproducible doping of SiC is generally accomplished *in situ* during epitaxial growth of the material [11]. The size of the nitrogen atom allows it to occupy either the C- or Si-site of the SiC lattice, but the C-site has generally been found to be preferred [50, 51]. In Paper **VI**, the adsorption of nitrogen-containing species onto the Si- and C-rich planes of SiC(0001) was theoretically studied by using DFT. The purpose was to investigate the mechanisms for N incorporation during epitaxial growth of *in situ* N-doped SiC. Thermodynamic calculations have earlier been performed for experimental conditions used under *in situ* nitrogen doping of SiC [52]. The results from those calculations were used as a guide to the gaseous composition above a growing SiC surface in the present theoretical study.

The adsorption of N_2, N, NH_3, NH_2, CN, HCN, HNC, H_2CNH, SiN, SiNH and Si_2N was, with three exceptions, found to be exothermic to both SiC surfaces. The exceptions include one-fold adsorption of (i) NH_3, or (ii) HCN or

HNC by the N atom to the C-plane of SiC(0001). The two-fold adsorption processes were all found to be exothermic and more favorable for the Si than for the C surface. Furthermore, adsorption by the N(Si) atom in the adsorbate was found to be stronger to the Si(C) surface, while the adsorbates seem to bind strongly to both surfaces by the C atom.

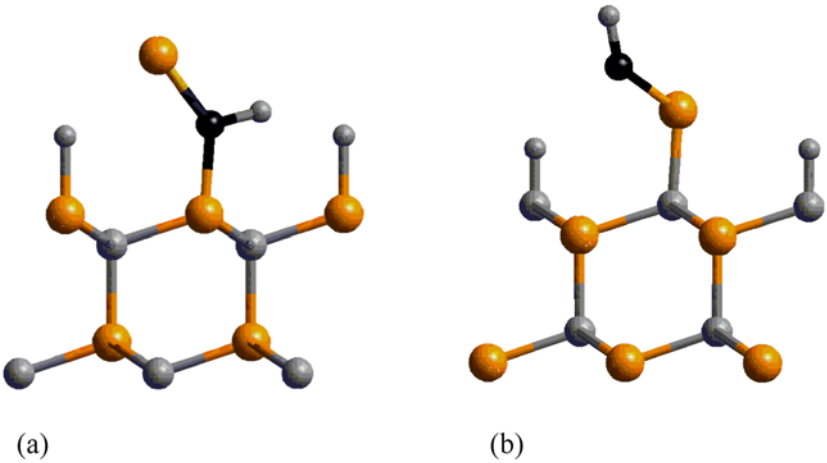

Figure 5.7: The bonding geometries for the adsorption of SiNH (a) by the N atom to the Si-rich plane and (b) by the Si atom to the C-rich plane of SiC(0001).

Reproducible *n*-type dopant incorporation (from below 10^{14} to 10^{19} cm^{-3}) into SiC has been obtained by using the site-competition epitaxial technique introduced by Larkin [53]. This technique is based on intentional variations of the C/Si ratio of the precursors during growth. The N incorporation has been found to decrease with an increased C/Si ratio despite a constant N_2-flow [52, 54]. The N-containing species are then generally believed to be ”out-competed” by a high concentration of the carbon growth species.

N_2, NH_3 and HCN are believed to be present in relatively high concentrations above the growing SiC surfaces. However, the adsorption processes of these species were not found to be very favorable. The SiNH species was, by thermodynamic calculations, also predicted to exist in the gaseous atmosphere during *in situ* growth of SiC and the adsorption of this species was more favorable compared to the other species investigated [52]. Moreover, SiNH adsorption was found to preferably occur by the N and Si atom to the Si- and C-rich planes of SiC(0001), respectively (Fig. 5.7). Adsorption of this species to either of the two surfaces would, hence, preferably place the N atom in a C site of the lattice, which has been found to be the favored site for N-incorporation into SiC [50, 51]. For increased C precursor concentrations, under which the N

incorporation generally has been found to be ”out-competed”, the SiNH concentration is lowered. Hence, a plausible explanation for the site-competition epitaxial technique is, according to Paper **VI**, that the N atom is implanted into the Si and C planes of the growing SiC material by adsorption of different atoms in the SiNH adsorbate.

5.4.3 Incorporation of contaminant species into h-BN

In a recent DFT investigation, oxygen (or nitrogen or carbon) interstitial defects have been predicted to induce a transformation of h-BN into c-BN [55]. This might be true under certain conditions, but the unintentional incorporation of contaminant species is practically a common problem for BN growth [6, 4]. As presented in Sec. 5.3.5, the BN films grown in Paper **V** were found to incorporate oxygen and carbon when exposed to ambient atmospheres. Moreover, the films were found to include a considerable amount of hydrogen during growth. The adsorption of H_2, O_2 and CO_2 to h-BN(100) edges was, for this reason, theoretically studied and compared with adsorption of BN growth species (Paper **IV**). As a result, an H radical was found to form bonds of similar strengths as the N-containing species (i.e., N, NH and NH_2) and the B-containing species (i.e., BBr and BBr_2) to the B-rich and N-rich edge of h-BN(100), respectively. However, adsorption of NH_3, BBr_3 and CO_2 was considerably weaker. O_2 was found to adsorb more strongly (compared to H) to the B-rich edge but only weakly to the N-rich edge. This implies that oxygen has a preference for binding to the B atoms in h-BN, and the more favorable source of oxygen is the O_2 molecule. H_2 molecules bound more strongly than H atoms to both h-BN(100) edges. The adsorption energies of hydrogen molecules and atoms were larger (by $\sim 10\%$) for the N-rich edge of h-BN(100). Moreover, the energy for B adsorption to the N-rich edge was of the same magnitude as the corresponding one for H_2 adsorption (Sec. 5.3.6). The energetics, hence, agrees with the experimental findings that the B and N atoms of h-BN have tendencies for binding to species containing oxygen and hydrogen, respectively.

Concluding remarks

Silicon carbide surfaces have been theoretically investigated by means of DFT. A (1x2) buckling reconstruction of the unterminated Si-rich SiC(0001) surface was then suggested, while only a downward relaxation was obtained for the C-rich surface. Abstraction reactions of the corresponding H-terminated surfaces were modelled by *ab initio* dynamics. The H-atoms were then found to bind strongly to the surfaces also at temperatures as high as 1600 and 2300 °C. Moreover, the size and shape were found to influence the reactions for a continued growth of SiC clusters.

Nitrogen-doped SiC, which is obtained *in situ* during growth, has been thoroughly studied, but the underlaying mechanism for N incorporation is not well understood. According to the present work, SiNH is a possible species by which the N-introduction occurs. N_2, NH_3 and HCN are probably more abundant under vapor growth conditions. The adsorption energies of these species were found only slightly exothermic or endothermic. However, some of them might become adsorbed if the corresponding reaction barriers are small enough. Barriers for adsorption as well as thermal effects of these processes would, hence, be of interest to study further.

A general understanding of BN growth by ALD has been obtained as a result of the present work. By photochemical dissociation of the gaseous precursors NH_3 and BBr_3, an increased growth rate and a somewhat more stable BN material was obtained for low deposition temperatures ($\sim$ 400 °C). The deposited films consisted of nanocrystalline grains of hexagonal BN and they were observed to be very smooth. The applied precursor species were theoretically confirmed to bind strongly to both the hexagonal and cubic modifications of growing BN surfaces. Moreover, only the NH_3 and BBr_3 molecules were found to preferably result in the cubic phase. There is much more to learn about this process and the various parameters (including substrate and precursor gases) must be further optimized in order to obtain a BN material with higher density. Moreover, for efficient coupling between theory and experiment, *in situ* surface analysis would be very valuable.

Acknowledgements

First, I want to thank Dr Karin Larsson for introducing me to the world of academic research. She has given me much encouragement and constructive criticism during the past five years.

Dr Mikael Ottosson has been very generous with experimental expertise and time. It has also been a pleasure to work with Dr Peter Heszler.

Many thanks to Professor Jan-Otto Carlsson for providing the excellent facilities at the Ångström Laboratory and for valuable advice when needed.

Dr Örjan Danielsson, Dr Urban Forsberg and Dr Jie Zhang at Linköping University are gratefully acknowledged for inspiring discussions about SiC.

Janne Bohlin gave essential assistance while building my ALD-reactor. Gunilla Lindh, Ulrika Bergvall, Katarina Israelsson, Nils-Olov Ersson, Anders Lund and Peter Lundström have been very helpful with many practical matters. Other colleagues who, aside from being friends, often volunteered to give me technical and administrative support are Marie Herstedt, Tobias Törndahl and Sami Amira.

During the work on my thesis, I came to know many of the lovely individuals in the Department of Materials Chemistry and I would like to thank them for creating such a friendly atmosphere.

Finally, I want to thank my family for their support and for always believing in me. Thanks go also to my friends, young and old, for filling up my spare time with all kinds of activities and for simply being around. You know who you are. I specifically want to mention my darling Jonas.

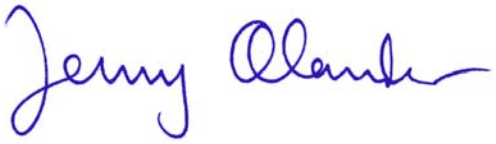

Jenny Olander, Uppsala the 24th of April 2003

Bibliography

[1] Bechstedt, F.; Käckell, P.; Zywietz, A.; Karch, K.; Adolph, B.; Tenelsen, K.; Furthmüller, J. *Phys. Stat. Sol. (b)* **1997,** *202,* 35.

[2] Bunshah, R. F. *Handbook of Hard Coatings;* Noyes Publications: New Jersey, 1st ed.; 2001.

[3] Byrappa, K.; Ohachi, T. *Crystal Growth Technology;* William Andrews Inc.: New York, 1st ed.; 2003.

[4] Paine, R. T.; Narula, C. K. *Chem. Rev.* **1990,** *90,* 73.

[5] Vel, L.; Demazeau, G.; Etourneau, J. *Mat. Sci. Eng* **1991,** *B10,* 149.

[6] Bartl, A.; Bohr, S.; Haubner, R.; Lux, B. *Int. J. Refract. Metals and Hard Mat.* **1996,** *14,* 145.

[7] Patibandla, N.; Luthra, K. *J. Electrochem. Soc.* **1992,** *139,* 3558.

[8] Zhang, X. W.; Boyen, H.-G.; Deyneka, N.; Ziemann, P.; Banhart, F.; Schreck, M. *Nature* **2003,** *1,* 1.

[9] Elliott, S. *The Physics and Chemistry of Solids;* Wiley: West Sussex, 1998.

[10] Thomas, J.; Weston, N. E.; O'Connor, T. *J. Amer. Chem. Soc.* **1963,** *84,* 4619.

[11] Davies, R.; Kelner, G.; Shur, M.; Palmour, J. W.; Edmond, J. A. *Proc. IEEE* **1991,** *79,* 677.

[12] Allendorf, M. D.; Kee, R. J. *J. Electrochem. Soc.* **1991,** *138,* 841.

[13] Konyashin, I.; Joachim, B.; Aldinger, F. *Chem. Vap. Dep.* **1997,** *3,* 239.

[14] Matsunami, H.; Kimoto, T. *Mat. Sci. Eng.* **1997,** *R20,* 125.

[15] Feldermann, H.; Ronning, C.; Hofsäss, H.; Huang, Y. L.; Seibt, M. *J. Appl. Phys* **2001,** *90,* 3248.

[16] Mårlid, B.; Larsson, K.; Carlsson, J.-O. *Phys. Rev. B* **2001,** *64,* 184107.

[17] Polo, M. C.; Sánchez, G.; Wang, W. L.; Esteve, J.; Andújar, J. L. *Appl. Phys. Lett* **1997,** *70,* 1682.

[18] Suntola, T.; Hyärinen, J. *Annu. Rev. Mat. Sci.* **1985,** *15,* 177.

[19] Sachev, H.; Haubner, R.; Nöth, H.; Lux, B. *Diam. Rel. Mater.* **1997,** *6,* 286.

[20] Zhang, W. J.; Jiang, X.; Matsumoto, S. *Appl. Phys. Lett.* **2001,** *79,* 27.

[21] Lin, M. E.; Strite, W.; Agarwal, A.; Salvador, A.; Zhou, G. L.; Teraguchi, N.; Rockett, A.; Moroç, H. *Appl. Phys. Lett.* **1993,** *62,* 702.

[22] Pollmann, J.; Krüger, P.; Sabisch, M. *Phys. Stat. Sol. B* **1997,** *202,* 421.

[23] Starke, U. *Phys. Stat. Sol. (b)* **1997,** *202,* 475.

[24] Kádas, K.; Kern, G.; Hafner, J. *Phys. Rev.* **2000,** *136,* B864.

[25] Osuch, K.; Verwoerd, W. *Surf. Sci.* **1996,** *345,* 75.

[26] van Elsbergen, V.; Janzen, O.; Münch, W. *Mat. Sci. Eng.* **1997,** *B46,* 366.

[27] Larsson, K.; Carlsson, J.-O. *J. Phys. Chem.* **1999,** *103,* 6533.

[28] Møller, C.; Plesset, M. S. *Phys. Rev.* **1934,** *46,* 618.

[29] Hohenberg, P.; Kohn, W. *Phys. Rev.* **1964,** *136,* B864.

[30] Parr, R. G.; Yang, W. *Density-Functional Theory of Atoms and Molecules;* Oxford University Press: New Yord, 1989.

[31] Kohn, W.; Sham, L. J. *Phys. Rev.* **1965,** *140,* A1133.

[32] Perdew, J.; Wang, Y. *Phys. Rev. B* **1992,** *45,* 13244.

[33] Perdew, J.; Zunger, A. *Phys. Rev. B* **1981,** *23,* 5048.

[34] Ashcroft, N. W.; Mermin, N. D. *Solid State Physics;* Holt Saunders: Philadelphia, 1976.

[35] Monkhorst, H.; Pack, J. D. *Phys. Rev. B* **1976,** *13,* 5188.

[36] Kleinman, L.; Bylander, D. *Phys. Rev. Lett.* **1982,** *48,* 1425.

[37] Fletcher, R. *Practical Methods of Optimization;* Wiley: New York, 1st ed.; 1980.

[38] Payne, M. C.; Teter, M. P.; Allan, D. C.; Arias, T. A.; Joannopoulus, J. D. *Rev. Mod. Phys.* **1992,** *64,* 1045.

[39] Verma, A. R. *Polymorphism and Polytypism in Crystals;* Wiley: New York, 1966.

[40] Nosé, S. *J. Chem. Phys.* **1984,** *81,* 511.

[41] Reuter, K.; Schardt, J.; Bernhardt, J.; Wedler, H.; Starke, U.; Heinz, K. *Phys. Rev. B* **1998,** *58,* 10806.

[42] Lespiaux, D.; Langlais, F. *Thin Solid Films* **1995,** *265,* 40.

[43] Tsuchida, H.; Kamata, I.; Izumi, K. *Jpn J. Appl. Phys.* **1997,** *36,* L699.

[44] Tsuchida, H.; Kamata, I.; Izumi, K. *Mat. Sci. Forum* **1998,** *264,* 351.

[45] Krauss, T. D.; Brus, L. E. *Phys. Rev. Lett.* **2001,** *83,* 3.

[46] Ohshita, Y. *J. Cryst. Growth* **1991,** *110,* 516.

[47] Ferguson, J. D.; Weimer, A. W.; George, S. M. *Thin Solid Films* **2002,** *413,* 16.

[48] Mårlid, B.; Ottosson, M.; Pettersson, U.; Larsson, K.; Carlsson, J.-O. *Thin Solid Films* **2002,** *402,* 167.

[49] Mårlid, B.; Larsson, K. *J. Phys. Chem. B* **1999,** *103,* 7637.

[50] Deák, P.; Gali, A.; Miro, J.; Guiterrez, R.; Sieck, A.; Frauenheim, T. *Mat. Sci. Forum* **1998,** *264-268,* 279.

[51] Woodbury, H. H.; Ludwig, G. W. *Phys. Rev.* **1961,** *124,* 1083.

[52] Forsberg, U.; Ö. Danielsson,; Henry, A.; Linnarsson, M. K.; Janzén, E. *J. Cryst. Growth* **2002,** *236,* 101.

[53] Larkin, D. J. *Phys. Stat. Sol. (b)* **1997,** *202,* 305.

[54] Kimoto, T.; Itoh, A.; Matsunami, H. *Appl. Phys. Lett.* **1995,** *67,* 2385.

[55] Mosuang, T.; Lowther, J. *Phys. Rev. B* **2002,** *66,* 014112.